Invitation to inverse problems
—working with real-world data—

Samuli Siltanen and Jennifer Mueller

August 11, 2026

Contents

Part I

When the data plays tricks on you

Chapter 5

Probing with electric currents

Later in the book we will explore Electrical Impedance Tomography, or EIT for short. EIT is an imaging method where the internal structure of a conductive body is recovered from electric boundary measurements. There are plenty of promising uses for EIT in medical imaging, nondestructive testing and industrial process monitoring. See Chapter **??** for more details on these applications.

This Chapter is intended to be a friendly introduction to the world of EIT. In Section 5.1.1 we briefly review basic electrical principles related to voltages, current flows and resistance. Section 5.1.2 is devoted to showing why EIT imaging of one-dimensional objets is not plausible. To that end we develop a simple linear diffusion model.

Then Section 5.2 moves on to diffusion models based on two-dimensional grids of pixels. We will see that such a construction serves as a reasonable coarse model of EIT imaging. However, the task of recovering the electric conductivity distribution from the electric boundary data is a nonlinear and severely ill-posed inverse problem. Therefore, making EIT work in a given application requires thorough understanding of the underlying mathematics. In this chapter we will lay groundwork for EIT by building pixel-based diffusion models. They are relatively simple but still can demonstrate the character and main challenges of EIT.

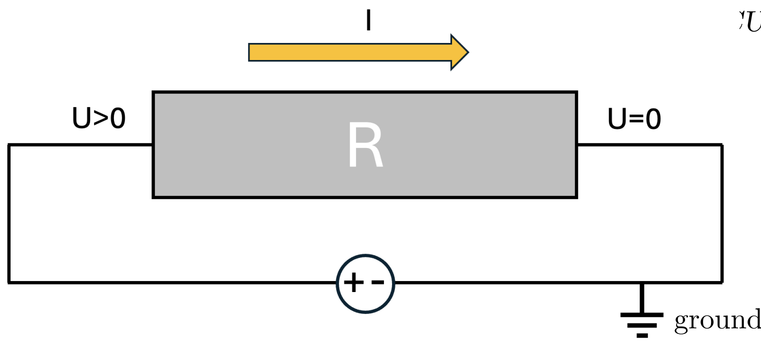

Figure 5.1: How a resistor works. There is a voltage difference over the resistor depicted as a gray rectangle. The disc with + and − denotes a battery of U volts. Ground denotes zero voltage potential, to which all other voltages are compared. So the voltage at the left lend of the resistor is $U > 0$, and the voltage at the right end is zero. Electric current through the resistor can be calculated from (5.1) to be $I = U/R$.

5.1 Diffusion models and electricity

5.1.1 Voltages, currents and resistors

We build mathematical models based on basic physics of electricity. Our starting point is Ohm's Law in the form

$$U = RI, \tag{5.1}$$

where U is the voltage difference over a resistor, I is the current through the resistor and R is electric resistance. Electric current runs from higher voltage potential towards lower; by convention, electrons flow against the current. Voltage U is measured in volts (V), current in amperes (A) and resistance in ohms (Ω). See Figure 5.1.

It is the tradition in EIT to consider conductance instead of resistance. Let us denote conductance by $G = 1/R$, measured in siemens $S = \Omega^{-1}$. In terms of conductance, Ohm's Law takes the form

$$I = GU. \tag{5.2}$$

Our aim is to build a *diffusion model* for simulating EIT measurements in a way requiring minimal mathematical background from the reader. The model is based on pixels. There will be a voltage potential value inside each pixel and a conductance value between the pixels. See Figure 5.3 for an illustration of formula (5.2) in the case of two pixels.

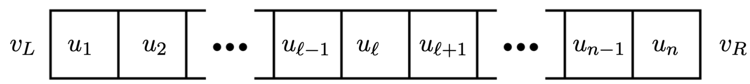

Figure 5.2: One-dimensional diffusion model with n pixels. The variables u_ℓ with $\ell = 1, 2, \ldots, n$ describe voltage in the pixels, and v_L, v_R are voltages at the left and right electrodes, respectively.

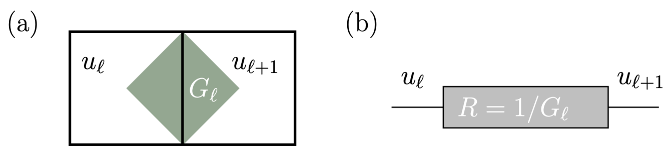

Figure 5.3: (a) Voltage potential in the left pixel is denoted by u_ℓ and the right one by $u_{\ell+1}$. We denote the electric conductance G_ℓ over the interface between the pixels as a diamond. Electric current from left to right can then be calculated using (5.2) to be $I_\ell = G_\ell(u_\ell - u_{\ell+1})$. (b) The same situation than (a), but expressed in terms of a resistor of resistance $R = 1/G_\ell$. The resulting electric current is the same in both cases.

5.1.2 One-dimensional diffusion model

Our diffusion model contains a horizontal linear array of n pixels as shown in Figure 5.2. The left edge of the leftmost pixel and the right edge of the rightmost edges are thought of as electrodes through which we inject currents. Voltages at the electrodes are denoted by v_L (left end) and v_R (right end). Variables $u_1, u_2, u_3, \ldots, u_n$ are voltages inside the pixels.

Our array of pixels is a coarse model of a rod of conductive material, allowed to be non-homogeneous. So we assign a conductance $G_\ell > 0$ to every vertical edge between neighboring pixels as shown in Figure 5.3. More precisely, the current flowing from pixel u_ℓ to $u_{\ell+1}$ can be calculated using (5.2) as

$$I_\ell = G_\ell(u_\ell - u_{\ell+1}), \qquad \ell = 1, 2, 3, \ldots, n-1. \tag{5.3}$$

This brings us to the central concept in diffusion models: the *balance equation*. Namely, Kirchhoff's current law states that the amount of electric current flowing into a pixel from left must equal the current exiting the pixel on the right. In mathematical terms, the balance equation for pixel ℓ is $I_{\ell-1} = -I_\ell$. Using (5.3) we get

$$G_{\ell-1}(u_{\ell-1} - u_\ell) = G_\ell(u_\ell - u_{\ell+1}), \qquad \ell = 2, 3, \ldots, n-1. \tag{5.4}$$

Equation (5.4) describes Kirchhoff's current law at all the internal pixels ($\ell = 2, 3, \ldots, n-1$) but not at pixels 1 and n. For those two we need to consider currents through the electrodes into the linear model. Unless otherwise stated, we will take the conductance at the outermost edges to be $G_0 = 1S = G_n$. So then the currents applied at the left and right ends are, ignoring units,

$$I_L = v_L - u_1, \qquad I_R = v_R - u_n. \tag{5.5}$$

Note that the sign convention for I_R is different from all other pixels. That is because with the applied boundary currents we want to think that *current flowing from outside into the rod is positive.*

Homogeneous three-pixel model

See Figure 5.4 for an example with $n = 3$ pixels and all conductances equal to 1. Figure 5.4(a) lists all the voltage variables involved, and Figure 5.4(b) shows the conductances. We will build a matrix model

$$A\vec{v} = A \begin{bmatrix} v_L \\ u_1 \\ u_2 \\ u_3 \\ v_R \end{bmatrix} = \vec{b}, \tag{5.6}$$

where A is a 5×5 matrix and the right hand side vector $\vec{b}$ depends on the current feeds.

Let's start building the matrix equation (5.6) by inserting the boundary conditions. They are given as current feeds (5.5), and we get the first two rows:

$$\begin{bmatrix} 1 & -1 & 0 & 0 & 0 \\ 0 & 0 & 0 & -1 & 1 \\ \cdot & \cdot & \cdot & \cdot & \cdot \\ \cdot & \cdot & \cdot & \cdot & \cdot \\ \cdot & \cdot & \cdot & \cdot & \cdot \end{bmatrix} \begin{bmatrix} v_L \\ u_1 \\ u_2 \\ u_3 \\ v_R \end{bmatrix} = \begin{bmatrix} I_L \\ I_R \\ \cdot \\ \cdot \\ \cdot \end{bmatrix}.$$

Next we go to internal balance equations. From (5.4) and the identities $G_1 = 1 = G_2$ we get the equation for the middle pixel: $u_1 - u_2 = u_2 - u_3$. That gives us row 4 in the matrix model:

$$\begin{bmatrix} 1 & -1 & 0 & 0 & 0 \\ 0 & 0 & 0 & -1 & 1 \\ \cdot & \cdot & \cdot & \cdot & \cdot \\ 0 & 1 & -2 & 1 & 0 \\ \cdot & \cdot & \cdot & \cdot & \cdot \end{bmatrix} \begin{bmatrix} v_L \\ u_1 \\ u_2 \\ u_3 \\ v_R \end{bmatrix} = \begin{bmatrix} I_L \\ I_R \\ \cdot \\ 0 \\ \cdot \end{bmatrix}.$$

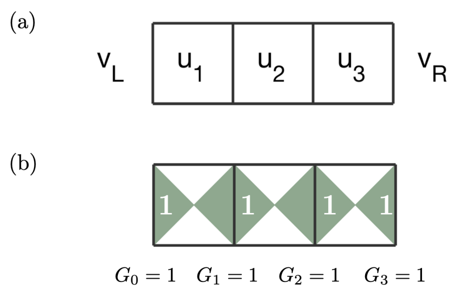

Figure 5.4: A homogeneous linear diffusion model with three pixels. (a) Voltages v_L and v_R are the ones we can measure at the ends of our pixelized rod. Inside the rod, there are three pixels with voltages u_1, u_2, u_3 that are not available for direct measurement. (b) Conductances between the pixels. Here all the conductances are equal to 1, including those at the "electrodes", namely the leftmost and rightmost edges between voltages v_L, u_1 and u_3, v_R, respectively.

Similar balance equations hold for pixels 1 and 3, with voltage potentials v_L and v_R appropriately inserted. These three equations fill the final three rows and complete the construction of our matrix model:

$$A\vec{v} = \left[\begin{array}{ccccc} 1 & -1 & 0 & 0 & 0 \\ 0 & 0 & 0 & -1 & 1 \\ \hline 1 & -2 & 1 & 0 & 0 \\ 0 & 1 & -2 & 1 & 0 \\ 0 & 0 & 1 & -2 & 1 \end{array}\right] \left[\begin{array}{c} v_L \\ u_1 \\ u_2 \\ u_3 \\ v_R \end{array}\right] = \left[\begin{array}{c} I_L \\ I_R \\ \hline 0 \\ 0 \\ 0 \end{array}\right]. \tag{5.7}$$

The horizontal lines in (5.7) indicate the two conceptually distinct blocks: top block for boundary data and bottom block for balance equations coming from Kirchhoff's current law.

A straightforward idea would be to invert the square matrix A to solve (5.7). But it is not that simple as A is a singular matrix: $\det(A) = 0$, so the inverse does not exist. Further analysis reveals that A has a one-dimensional kernel:

$$\ker(A) = \{[\lambda, \lambda, \lambda, \lambda, \lambda]^T \in \mathbb{R}^5 \mid \lambda \in \mathbb{R}\}.$$

This means non-uniqueness in the following sense. If a vector $\vec{v}$ is a solution of (5.7), then any vector $\vec{v}_0 \in \ker(A)$ produces another solution $\vec{v} + \vec{v}_0$. So (5.7) has infinitely many solutions, and we need a way to pick out the one we want.

One approach is to ground the right electrode, setting the voltage potential there to zero:

$$v_R = 0. \tag{5.8}$$

Let's see how this works in a concrete example. Consider feeding a current $I_L = 1$ (mA) into the rod through the left electrode and taking the current out form the right electrode: $I_R = -1$. First calculate the least-squares solution as

$$\vec{v}^\dagger = (A^T A)^\dagger A^T \begin{bmatrix} 1 \\ -1 \\ 0 \\ 0 \\ 0 \end{bmatrix}.$$

Then the "grounding of the right electrode", in other words enforcing (5.8) can be modelled like this:

$$\vec{v}_\perp = \vec{v}^\dagger - \begin{bmatrix} v_R^\dagger \\ v_R^\dagger \\ v_R^\dagger \\ v_R^\dagger \\ v_R^\dagger \end{bmatrix} = \begin{bmatrix} v_L^\dagger - v_R^\dagger \\ u_1^\dagger - v_R^\dagger \\ u_2^\dagger - v_R^\dagger \\ u_3^\dagger - v_R^\dagger \\ 0 \end{bmatrix}.$$

We get the unique solution $\vec{v}_\perp = [4, 3, 2, 1, 0]^T$, as shown in in Figure 5.5. Our measurement data will be just one number: voltage v_L at the left electrode. We have $v_L = 4$ millivolts.

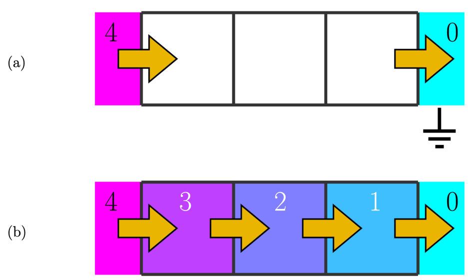

Figure 5.5: Feeding current to the linear diffusion model shown in Figure 5.4. (a) View of the boundary measurements. We know the currents at both electrodes, and the right electrode is grounded, so $v_R = 0$. The voltage at the left electrode is measured to be $v_L = 4$ mV. (b) A peek under the hood. The voltages inside the pixels are not available for measurements, but in a simulated model we can study them. There is a voltage drop of 1 mV between every pixel, resulting in 1 mA current in each case since the conductance is 1 everywhere.

(a)

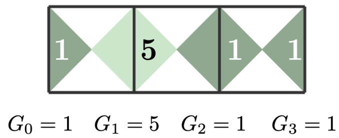

(b)

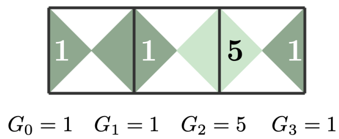

Figure 5.6: Our two non-homogeneous conductivity distributions for the three-pixel diffusion model. Conductances at the electrodes equal one. (a) Internal conductances are $G_1 = 5$ Siemens and $G_2 = 1$ Siemens. (b) Internal conductances are $G_1 = 1$ Siemens and $G_2 = 5$ Siemens.

Non-uniqueness in the three-pixel model

Having conquered the homogeneous three-pixel case in the previous section, we now introduce changes in the conductive interior of the rod. See Figure 5.6 for our two digital phantoms, where we insert a higher conductance $G = 5$ Siemens to one of the two internal edges in the model. Can we recover the conductance values from boundary measurements?

Let us derive a matrix model similar to (5.7) for the case in Figure 5.6(a). The two first rows in the system stay the same. From $G_1 = 5$ we get the balance equation for the left pixel:

$$(v_L - u_1) = 5(u_1 - u_2) \quad \Rightarrow \quad v_L - 6u_1 + 5u_2 = 0.$$

A similar calculation for the middle pixel gives

$$5(u_1 - u_2) = u_2 - u_3 \quad \Rightarrow \quad 5u_1 - 6u_2 + u_3 = 0.$$

The last row is the same as in (5.7). So we get

$$\begin{bmatrix} 1 & -1 & 0 & 0 & 0 \\ 0 & 0 & 0 & -1 & 1 \\ 1 & -6 & 5 & 0 & 0 \\ 0 & 5 & -6 & 1 & 0 \\ 0 & 0 & 1 & -2 & 1 \end{bmatrix} \begin{bmatrix} v_L \\ u_1 \\ u_2 \\ u_3 \\ v_R \end{bmatrix} = \begin{bmatrix} 1 \\ -1 \\ 0 \\ 0 \\ 0 \end{bmatrix}, \tag{5.9}$$

whose solution including the grounding trick (5.8) is $\vec{v}_\perp = [3.2 \;\; 2.2 \;\; 2 \;\; 1 \;\; 0]^T$. Our measurement data is then 3.2 millivolts. See Figure 5.7 for the result.

Next step is to build the matrix model for case in Figure 5.6(b). We get

$$\begin{bmatrix} 1 & -1 & 0 & 0 & 0 \\ 0 & 0 & 0 & -1 & 1 \\ 1 & -2 & 1 & 0 & 0 \\ 0 & 1 & -6 & 5 & 0 \\ 0 & 0 & 5 & -6 & 1 \end{bmatrix} \begin{bmatrix} v_L \\ u_1 \\ u_2 \\ u_3 \\ v_R \end{bmatrix} = \begin{bmatrix} 1 \\ -1 \\ 0 \\ 0 \\ 0 \end{bmatrix}. \tag{5.10}$$

The solution is $\vec{v}_\perp = [3.2 \;\; 2.2 \;\; 1.2 \;\; 1 \;\; 0]^T$. Our measurement data is again $v_L = \vec{v}_1 = 3.2$ millivolts. See Figure 5.8 for the result.

Our conclusion is that current-to-voltage measurements at the ends of the rod cannot reveal details in the internal conductivity distribution within the rod. Namely, both cases (a) and (b) in Figure 5.6 lead to exactly the same measurement $v_L = 3.2$mV after the injection of 1mA of electric current.

What is happening? Note that that by (5.1) we have $(v_L - v_R) = RI$, where R is the total resistance of our pixelized rod. Now due to grounding we have $v_R = 0$, so our measurement is $v_L = RI$. Let's calculate the total resistance R. We know that the cumulative resistance of a series of resistors is just the sum of individual resistances, and that resistance is the inverse of conductance: $R_\ell = 1/G_\ell$. We arrive at

$$v_L = RI = (1 + \frac{1}{G_1} + \frac{1}{G_2} + 1)I.$$

Now we are ready to see that

$$\begin{aligned} v_L &= (1\Omega + \frac{1}{5}\Omega + 1\Omega + 1\Omega)1mA \\ &= (1\Omega + 1\Omega + \frac{1}{5}\Omega + 1\Omega)1mA \\ &= 3.2\Omega \cdot 1mA \\ &= 3.2mV. \end{aligned}$$

Mathematically speaking, it is the commutativity of addition that leads to nonuniqueness and makes EIT impossible in dimension one.

Therefore we next move to studying a diffusion model in dimension two, which is more interesting and actually describes a setup relevant to many imaging applications.

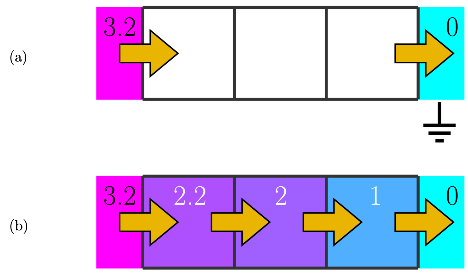

Figure 5.7: Feeding current to the linear diffusion model shown in Figure 5.6(a), where the internal conductances are $G_1 = 5$ and $G_2 = 1$. (a) The voltage at the left electrode is measured to be $v_L = 3.2$ mV. (b) Internal voltages revealed.

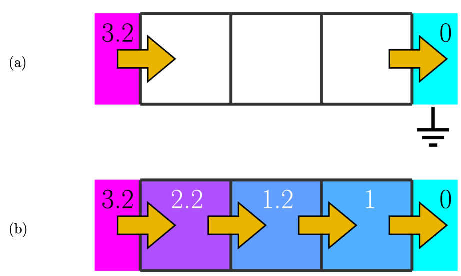

Figure 5.8: Feeding current to the linear diffusion model shown in Figure 5.6(b), where the conductances are $G_1 = 1$ and $G_2 = 5$. (a) The voltage at the left electrode is measured to be $v_L = 3.2$ mV. (b) Internal voltages revealed.

5.2 Two-dimensional diffusion model for EIT data

Consider the flow of electricity between one central pixel and its neighbors on the North, West, South and East sides as shown in Figure 5.9(a). We allow distinct conductances between the central pixel and the neighbors; let's call them G_N, G_W, G_S, G_E and draw them as green diamonds as in Figure 5.9(b).

The diffusion model is based on requiring conservation of charge: total sum of electric current into the central pixel should be zero. Taking the Northern neighbor as an example, we adapt formula (5.3) to give the current from the North towards the center as $I_N = G_N(u_N - u)$. The other neighbors have the same formula with the index N replaced by the appropriate one. We arrive at the balance equation

$$\begin{aligned} 0 &= I_W + I_S + I_E + I_N \\ &= G_W(u_W - u) + G_S(u_S - u) + G_E(u_E - u) + G_N(u_N - u) \end{aligned} \tag{5.11}$$

See Figure 5.9(c) for an illustration of four electric currents towards the center.

Our general model consists of an $n \times n$ grid of pixels with current flows satisfying (5.11) everywhere. There are also pixels at the boundary, and their outward edges will be treated as electrodes. Currents over those edges are specified by the person doing EIT imaging, contributing to the balance equations of the form (5.11), with slight adaptations at the corners.

5.2.1 Matrix equation for the general $n \times n$ grid

Pixel grid and variables

We consider a two-dimensional grid of $n \times n$ pixels with $n > 2$ an odd integer. Why should n be odd? well, everything would work just fine with even numbers as well, but with an odd n we have a unique "three o'clock pixel" where we can conveniently start electrode numbering. There are two kinds of variables in our model:

1. Voltages u_j at the pixels, $j = 1, 2, \ldots, n^2$.

2. Voltages v_i measured at the electrodes. We consider each outer edge of a boundary pixel to be an electrode. The corner pixels have one electrode each, modelled by the union of the two edges at the boundary of the model square. The indexing runs like this: $i = 1, 2, \ldots, L$ with $L = 4(n - 1)$.

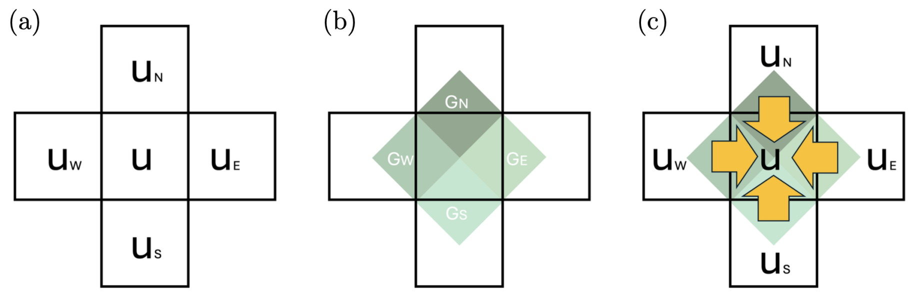

Figure 5.9: Modelling electricity flow between neighboring pixels in a two-dimensional grid. (a) Let's call the voltage at the center pixel u and name the neighboring pixels North, West, South and East. The voltages in those pixels are modelled by variables u_N, u_W, u_S, u_E. (b) Conductances between pixels are denoted by green diamonds. The higher the conductance, the lighter the green color. We call the conductances G_N, G_W, G_S, G_E. (c) Current flows between the center pixel and the four neighbors should sum up to zero according to formula (5.11).

See Figure 5.10 for three examples of our system for naming variables. Electrodes are numbered in a counter-clockwise manner, starting from the "three o'clock" electrode which is the outside edge of the middle pixel of the right-most column. The internal voltages are numbered column-wise following the Matlab convention.

Current patterns

In the one-dimensional diffusion model discussed in Section 5.1.2 we pushed electric current into the model through one end and took the current out from the other end. Here in two dimensions we have much more freedom for current feeds. We can choose the magnitude and direction of current independently at every electrode, with only a slight restriction: conservation of charge dictates that the sum of currents into the grid must be zero.

If our EIT setup has L electrodes, then we describe the currents applied through electrodes as a nonzero vector $\vec{I} \in R^L$ called a *current pattern*. Recall that in our $n \times n$ diffusion model we have $L = 4(n-1)$ electrodes. A positive element $\vec{I_\ell} > 0$ means that current is going into the domain through electrode ℓ, and a negative $\vec{I_\ell} < 0$ indicates that current of amplitude $|\vec{I_\ell}|$ amperes is exiting the domain through electrode ℓ. Due to conservation of

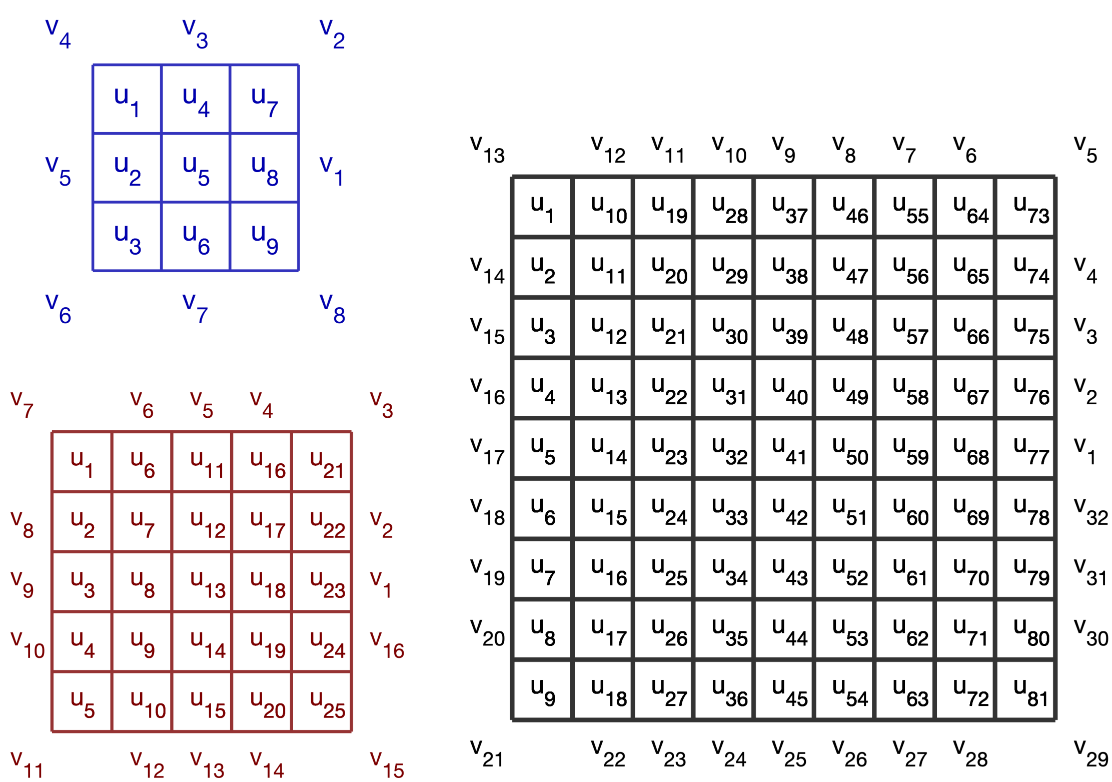

Figure 5.10: Variable numbering in the two-dimensional pixel diffusion models. Voltages v_i are measured at the electrodes. Internal voltages u_j are not available for direct observation in EIT, but their values are solved for in the simulation process. Top left in blue: the 3×3 pixel case. Bottom left in red: the 5×5 pixel case. Right: the 9×9 pixel case. This is especially interesting as the number of electrodes is 32, a common design choice in practical EIT devices.

charge it holds that

$$\sum_{\ell=1}^{L} \vec{I}_\ell = 0.$$

Therefore, we have at most $L-1$ linearly independent current patterns.

Building the linear system

There are two types of equations in our diffusion models: boundary conditions describing the currents fed through the boundary, and balance equations of the form (5.11) for all pixels in the grid. The equations will be collected into a matrix model

$$A\vec{v} = \vec{b}, \tag{5.12}$$

where $\vec{v} = [v_1, \ldots, v_L, u_1, \ldots, u_{n^2}]^T \in \mathbb{R}^N$ with $N = n^2 + L = n^2 + 4(n-1)$ and A is a square matrix of size $N \times N$. The right hand side vector $\vec{b} \in \mathbb{R}^N$ contains zeros for all balance equations of internal pixels and elements depending on the current feeds in case of boundary pixels.

$$A\vec{v} = \left[\begin{array}{c|c} I & A' \\ \hline A'' & A''' \end{array}\right] \left[\begin{array}{c} v_1 \\ \vdots \\ v_L \\ \hline u_1 \\ \vdots \\ u_{n^2} \end{array}\right] = \left[\begin{array}{c} b_1 \\ \vdots \\ b_L \\ \hline 0 \\ \vdots \\ 0 \end{array}\right] = \vec{b}, \tag{5.13}$$

where I is the $L \times L$ identity matrix and A', A'', A''' are block matrices of appropriate sizes. Boundary conditions, in this case current feeds, are described in block A'. Blocks A'' and A''' contain balance equations of type (5.11).

We will discuss a specific case of constructing equation (5.13) in detail in Section 5.2.2.

Unique solution for the matrix equation

Recall that in the one-dimensional model discussed in Section 5.1.2 we grounded one of the electrodes, making the solution unique. Without the grounding, the solution was only unique up to a constant. This is because electric voltage potential is not an absolute physical quantity but rather something we always need to compare to a reference value called ground. How do we deal with this in the two-dimensional case?

We could again ground one electrode, call the voltage there zero, and specify the voltages everywhere else by difference to the ground. But we do something different. The reason for this is that we want to be better aligned with the partial differential equation models for EIT discussed later in Chapter **??**.

The matrix A in (5.12) will indeed have a kernel of dimension one. So the solution of (5.12) is unique up to a constant, and we can find some representative of the solution space by solving (5.12) in the least squares sense for the minimum norm solution. Recall that a vector $\vec{w}$ is called a *least-squares solution* of the equation $A\vec{v} = \vec{b}$ if

$$\|A\vec{w} - \vec{b}\| = \min_{\vec{v}} \|A\vec{v} - \vec{b}\|. \tag{5.14}$$

Furthermore, a least-squares solution $\vec{v}^+$ is called the *minimum norm solution* if

$$\|\vec{v}^+\| = \inf\{\|\vec{w}\| \,:\, \vec{w} \text{ is a least-squares solution of } A\vec{v} = \vec{b}\}. \tag{5.15}$$

The minimum norm solution can be defined constructively using the singular value decomposition (SVD), as explained in [**?**, Chapter 4]. Numerical software packages have optimized algorithms for calculating minimum norm solutions.

So what do we do instead of grounding an electrode? Denote the voltage potentials given by the minimum norm solution at all the pixels and electrodes by

$$\vec{v}^+ = [v_1^+, \ldots, v_L^+, u_1^+, \ldots, u_{n^2}^+]^T$$

and calculate the mean value of the electrode voltages:

$$\overline{v} = \frac{1}{L}\sum_{j=1}^{L} v_j^+.$$

Then we simply subtract $\overline{v}$ from all the voltages in the solution:

$$\vec{v} = \vec{v}^+ - \overline{v}. \tag{5.16}$$

This method finds the unique solution of (5.12) with voltages at the electrodes summing up to zero.

The current-to-voltage matrix

Now consider applying the current pattern I^j and calculating the corresponding unique solution $\vec{v}^{(j)} = [v_1^{(j)}, \ldots, v_L^{(j)}, u_1^{(j)}, \ldots, u_{n^2}^{(j)}]^T$ as shown in (5.16). Truncating the solution so that only the electrode voltages remain, we define

$$V^j := \begin{bmatrix} v_1^{(j)} \\ \vdots \\ v_L^{(j)} \end{bmatrix}.$$

It is a linear process to go from the applied current vector I^j to the measured voltage vector V^j. Therefore, there must be a current-to-voltage matrix R_γ of size $L \times L$ that satisfies $V^j = R_\gamma I^j$.

Furthermore, assume that we have chosen a set of $L-1$ linearly independent current patterns. Define the *current matrix* $\mathbf{I} \in \mathbb{R}^{L\times(L-1)}$ and voltage matrix $\mathbf{U} \in \mathbb{R}^{L\times(L-1)}$ by

$$\mathbf{I} := [I^1, I^2, \ldots, I^{(L-1)}], \qquad \mathbf{U} := [V^1, V^2, \ldots, V^{(L-1)}].$$

We arrive at the formula

$$\mathbf{U} = R_\gamma \mathbf{I}. \tag{5.17}$$

It is often useful to think of R_γ as the EIT data. Note that equation (5.17) is kind of an Ohm's law (5.1) for EIT.

In the next sections we study some particular cases of the general model.

5.2.2 Nonlinearity of EIT

We illustrate the nonlinear nature of the EIT inverse problem using 3×3 pixel diffusion models. Section 5.2.2 on the homogeneous model serves as background, and the actual example showing nonlinearity is presented in Section 5.2.2.

Homogeneous 3×3 pixel model

Presented in Chapter 3 was arguably the simplest possible mathematical model for X-ray tomography. There the object under imaging is a 2×2 pixel grid, probed by four X-ray measurements modelled as row and column sums of the attenuation matrix.

Here we attempt to do a similar thing for the nonlinear imaging modality called Electrical Impedance Tomography (EIT). There is a fundamental difference between EIT and X-ray tomography. X-rays always travel along straight lines, fixing the geometry of the measurement model and leading to a linear inverse problems. In EIT, the thing we want to image, namely electrical conductivity distribution, actually affects the paths of the probing energy, which is the electric current vector field.

Our 3×3 pixel model is extremely simple but is able to capture the non-liear aspect of EIT imaging. Perhaps it could be done even with a 2×2 pixel grid, but we feel that the 3×3 story is more expressive and compelling.

See the top left diagram in Figure 5.10 for the numbering of variables in the 3×3 pixel diffusion model. We take all the conductances between pixels to be 1. Equation (5.12) then takes the form

$$\left[\begin{array}{cccccccc|ccccccccc}
1&0&0&0&0&0&0&0&0&0&0&0&0&0&0&-1&0\\
0&1&0&0&0&0&0&0&0&0&0&0&0&0&-1&0&0\\
0&0&1&0&0&0&0&0&0&0&0&-1&0&0&0&0&0\\
0&0&0&1&0&0&0&0&-1&0&0&0&0&0&0&0&0\\
0&0&0&0&1&0&0&0&0&-1&0&0&0&0&0&0&0\\
0&0&0&0&0&1&0&0&0&0&-1&0&0&0&0&0&0\\
0&0&0&0&0&0&1&0&0&0&0&0&0&-1&0&0&0\\
0&0&0&0&0&0&0&1&0&0&0&0&0&0&0&0&-1\\
\hline
0&0&0&-1&0&0&0&0&3&-1&0&-1&0&0&0&0&0\\
0&0&0&0&-1&0&0&0&-1&4&-1&0&-1&0&0&0&0\\
0&0&0&0&0&-1&0&0&0&-1&3&0&0&-1&0&0&0\\
0&0&-1&0&0&0&0&0&-1&0&0&4&-1&0&-1&0&0\\
0&0&0&0&0&0&0&0&0&-1&0&-1&4&-1&0&-1&0\\
0&0&0&0&0&0&-1&0&0&0&-1&0&-1&4&0&0&-1\\
0&-1&0&0&0&0&0&0&0&0&0&-1&0&0&3&-1&0\\
-1&0&0&0&0&0&0&0&0&0&0&0&-1&0&-1&4&-1\\
0&0&0&0&0&0&0&-1&0&0&0&0&0&-1&0&-1&3
\end{array}\right]
\left[\begin{array}{c}
v_1\\ v_2\\ v_3\\ v_4\\ v_5\\ v_6\\ v_7\\ v_8\\ \hline u_1\\ u_2\\ u_3\\ u_4\\ u_5\\ u_6\\ u_7\\ u_8\\ u_9
\end{array}\right]
=
\left[\begin{array}{c}
-1\\ 0\\ 0\\ 0\\ 1\\ 0\\ 0\\ 0\\ \hline 0\\ 0\\ 0\\ 0\\ 0\\ 0\\ 0\\ 0\\ 0
\end{array}\right],$$

where the upper block of the matrix implements boundary conditions and the lower block enforces the balance equation (5.11) for each pixel. The unique solution whose electrode voltages sum up to zero is shown in Figure 5.11.

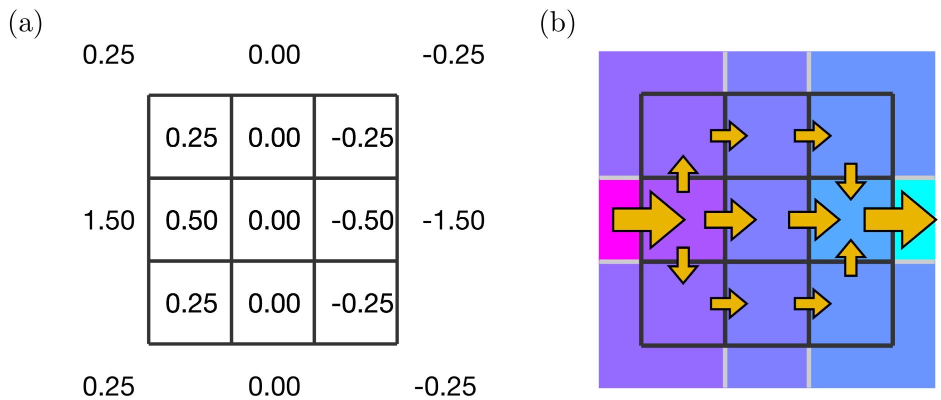

Figure 5.11: Solution of the homogeneous 3×3 pixel diffusion model. (a) Voltages as numbers. You can check that the electrode voltages sum up to zero. (b) Solution as colors, showing also the currents. Note that every pixel has some current going through it.

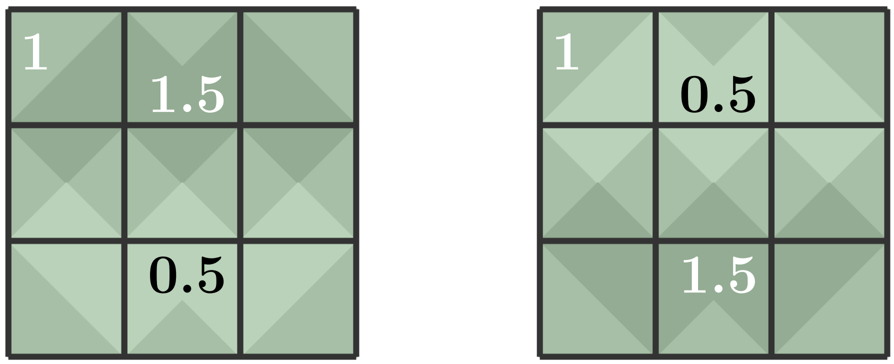

Figure 5.12: Two nonhomogeneous conductivity distributions. Dark green diamond means that the conductance between two pixels is 0.5. Light green color denotes conductance 1.5, and everywhere else the conductance is 1, depicted as an intermediate shade of green. Crucially for our nonlinearity demonstration, the edge-wise sum of these two distributions is a homogeneous conductivity having conductance 2 everywhere.

Nonlinearity in the 3×3 diffusion model

Our example is based on the two nonhomogeneous conductivity distributions shown in Figure 5.12. Both digital phantoms have edges with conductances 0.5, 1, and 1.5, distributed in such a way that their sum is 2 everywhere.

We simulate EIT measurements for both of those, and also for the homogeneous case with conductance 2, and observe that the measurements do not behave linearly. See Figure 5.13. This means that the task of recovering the conductances between pixels from electric boundary measurements is a nonlinear inverse problem.

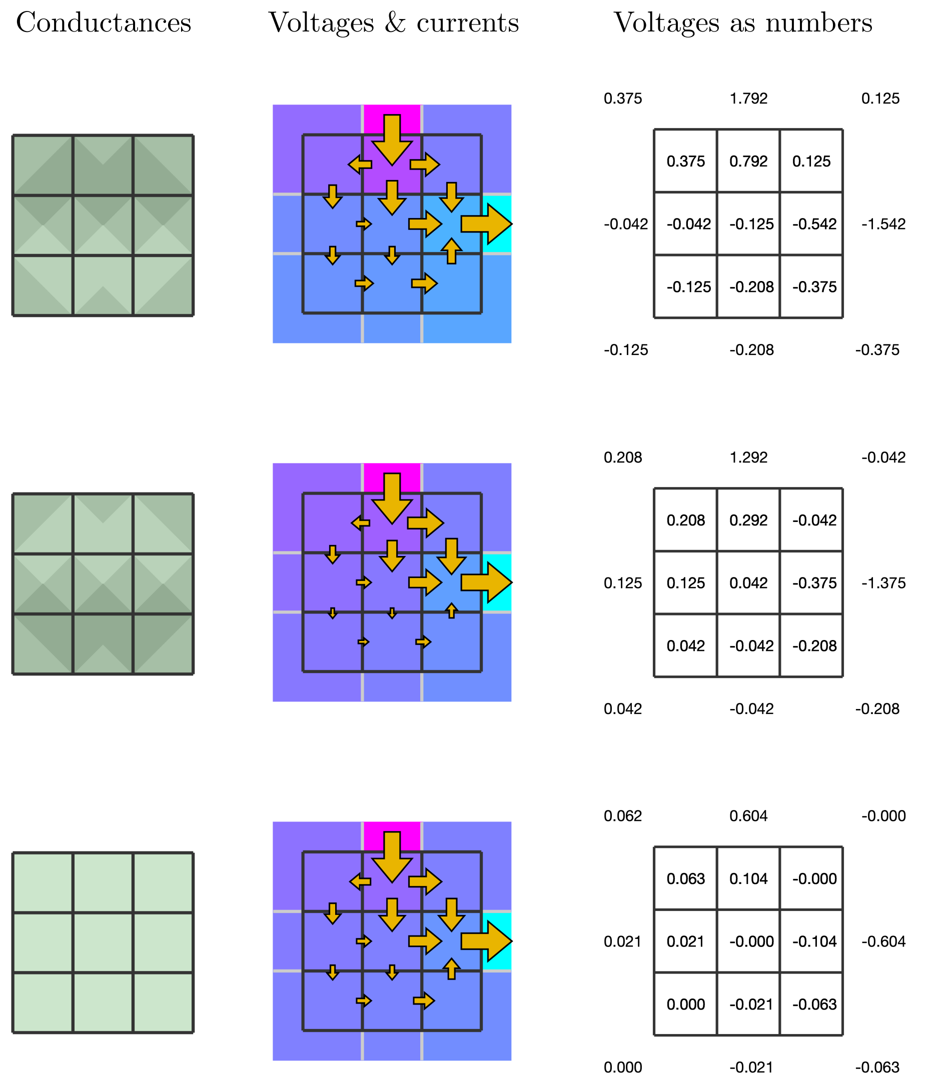

Figure 5.13: Nonlinearity demo. The two upper conductivity distributions in the left column sum up to the bottom conductivity distribution, which has constant conductance 2 everywhere. See Figure 5.12. The middle column shows the currents and voltages that result from the *exactly same* current feed pattern applied to each of the three examples. The right column records the voltages at the electrodes and at the internal pixels in our diffusion model. Note that the voltages in the right column do not sum up although the conductances in the left column do. This demonstrates that EIT is a nonlinear imaging modality.

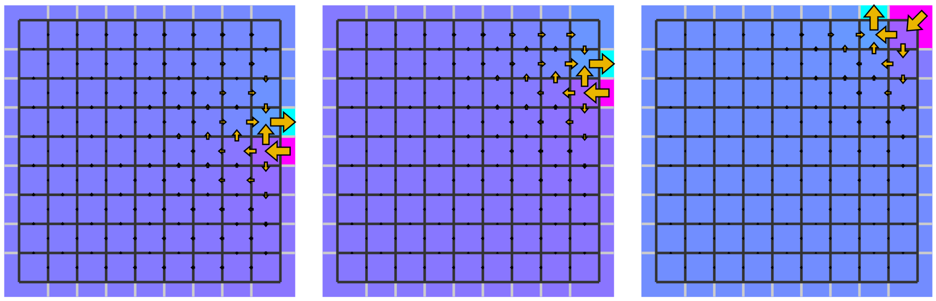

Figure 5.14: Solutions with a few adjacent current patterns in the case of the homogeneous conductivity one. The patterns are, from left to right, I^1, I^3 and I^5.

5.2.3 Ill-posedness of EIT

We use the 9×9 pixel grid whose numbering is shown on the right in Figure 5.10. It has $L = 32$ electrodes, a number seen in many actual EIT devices.

Adjacent current patterns

Here we concentrate on so-called *adjacent current patterns*, defined as the following $L - 1 = 31$ linearly independent vectors:

$$\begin{array}{rcl} I^1 & = & [1, -1, \ 0, \ 0, \ 0, \dots, \ 0, \ 0, \ 0]^T \in \mathbb{R}^{32}, \\ I^2 & = & [0, \ 1, -1, \ 0, \ 0, \dots, \ 0, \ 0, \ 0]^T \in \mathbb{R}^{32}, \\ I^3 & = & [0, \ 0, \ 1, -1, \ 0, \dots, \ 0, \ 0, \ 0]^T \in \mathbb{R}^{32}, \\ & \vdots & \\ I^{30} & = & [0, \ 0, \ 0, \ 0, \ 0, \dots, \ 1, -1, \ 0]^T \in \mathbb{R}^{32}, \\ I^{31} & = & [0, \ 0, \ 0, \ 0, \ 0, \dots, \ 0, \ 1, -1]^T \in \mathbb{R}^{32}. \end{array} \tag{5.18}$$

The idea of the adjacent pattern I^ℓ is that we feed current into the domain through electrode ℓ and take the current out through electrode $\ell + 1$.

Applying one of the current patterns results in voltages at the electrodes given by the values of the variables $v_1, \dots, v_{32}$, as described in Section 5.2.1. See Figure 5.14 for some example solutions. Using the current-to-voltage matrix notation, we have

$$I^j = \begin{bmatrix} I_1^j \\ I_2^j \\ \vdots \\ I_{32}^j \end{bmatrix} \mapsto R_\gamma \begin{bmatrix} I_1^j \\ I_2^j \\ \vdots \\ I_{32}^j \end{bmatrix} = \begin{bmatrix} v_1 \\ v_2 \\ \vdots \\ v_{32} \end{bmatrix} = V^j.$$

(a) (b)

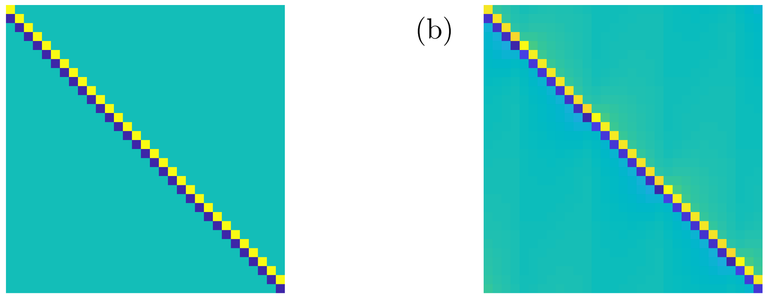

Figure 5.15: (a) Adjacent current matrix $\mathbf{I}^{\mathrm{adj}}$ defined in (5.19) for the case of 9×9 pixels and 32 electrodes. (b) The corresponding voltage matrix $\mathbf{U}^{\mathrm{adj}}$ in the case of constant conductivity distribution having all conductances equal to one.

We can collect all the adjacent current patterns in a matrix as columns:

$$\mathbf{I}^{\mathrm{adj}} = [I^1\ I^2 \dots I^{31}]. \tag{5.19}$$

See Figure 5.15(a). Similarly we define the voltage matrix

$$\mathbf{U}^{\mathrm{adj}} := [V^1\ V^2 \dots V^{31}],$$

shown in Figure 5.15(b).

Measuring details deep in the domain

We build up a simulated framework for studying EIT measurements of conductance details near the boundary and deeper in the domain. Spoiler: the deeper the inclusion is in the domain, the less the EIT measurement differs from that of a homogeneous target. This phenomenon was observed and analysed already in the 1980's [**?**, **?**].

Our starting point is the homogeneous 9×9 pixel diffusion model where all conductances are equal to 1 Siemens. You can see the result in Figure 5.15. Next we construct a series of examples, where the conductance at exactly one interface between two horizontally neighboring pixels is increased to 5 Siemens. In the left column of Figure 5.16 you can see how the higher-conductance inclusion is moving gradually deeper into the domain.

The middle column in Figure 5.16 shows the voltage matrices

$$\mathbf{U}_0^{\mathrm{adj}}, \mathbf{U}_1^{\mathrm{adj}}, \mathbf{U}_2^{\mathrm{adj}}, \mathbf{U}_3^{\mathrm{adj}}, \mathbf{U}_4^{\mathrm{adj}}, \mathbf{U}_5^{\mathrm{adj}}$$

resulting from applying the adjacent current patterns (5.18) to the six conductivity distributions, with $\mathbf{U}_0^{\mathrm{adj}}$ coming from the homogeneous one.

Images in the rightmost column in Figure 5.16 show the difference images

$$\mathbf{U}_0^{\mathrm{adj}} - \mathbf{U}_j^{\mathrm{adj}}, \qquad j = 1, 2, 3, 4, \tag{5.20}$$

between the voltage matrices of the homogeneous and the 5 nonhomogeneous cases. As a quantitative measure we also include the relative errors

$$E_j^{\infty} := \frac{\|\mathbf{U}_0^{\mathrm{adj}} - \mathbf{U}_j^{\mathrm{adj}}\|_\infty}{\|\mathbf{U}_0^{\mathrm{adj}}\|_\infty} \cdot 100\%, \qquad j = 1, 2, 3, 4. \tag{5.21}$$

Recall that for a general matrix $A = [a_{ij}]$, the sup norm is defined by $\|A\|_\infty = \max_{i,j} |a_{ij}|$.

Assume that our voltage measurements are corrupted by random noise with relative amplitude ε. Now, if an entry $\mathbf{U}_j^{\mathrm{adj}}(i,j)$ differs from $\mathbf{U}_0^{\mathrm{adj}}(i,j)$ by less than ε, we cannot distinguish the conductivity inclusion from homogeneous background in that data point. We introduce another quantitative measure of accuracy:

$$\mathcal{N}_j^{\varepsilon} = \#\big\{(i,j) \,\big|\, |\mathbf{U}_0^{\mathrm{adj}}(i,j) - \mathbf{U}_j^{\mathrm{adj}}(i,j)| > \varepsilon\big\}. \tag{5.22}$$

This is the number of data points in our measurement that are large enough to stand out amongst the noise. See Table 5.1 for the amounts of relevant data when the inclusion goes deeper.

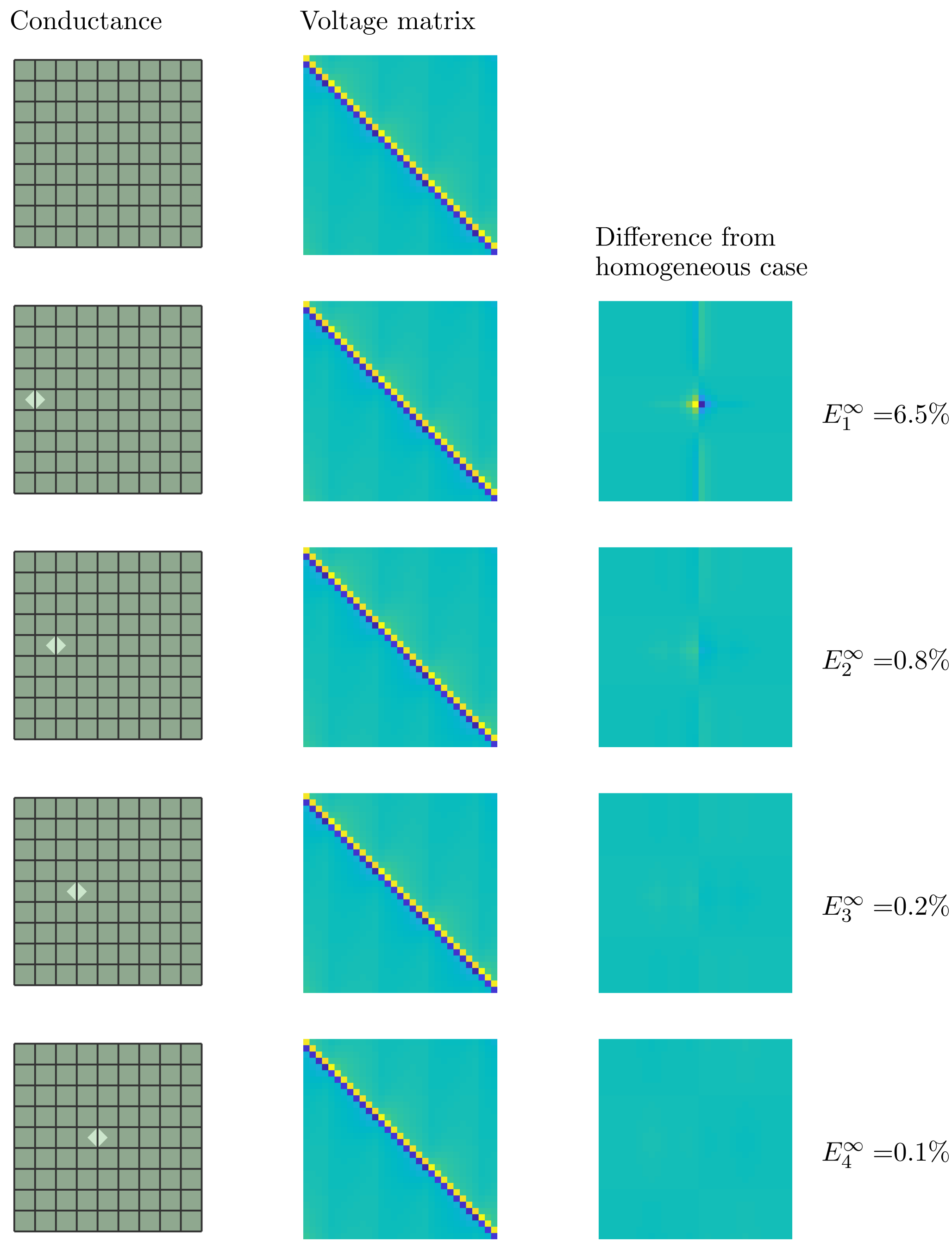

Figure 5.16: Ill-posedness demo. Top left: homogeneous conductivity distribution where all conductances between pixels are one. Top middle: voltage matrix measured from the homogeneous case when adjacent current patterns are applied. The same voltage matrix is shown in Figure **??**. Rows 2–5 show conductivities where a single inclusion (one interface with conductance 5 Siemens) is placed progressively deeper into the domain. The right column shows differencew images defined in (5.20). Note that the deeper the inclusion is located, the closer the measurement gets to the homogeneous case. The percentage shows the maximal relative absolute difference E_j^∞ between the voltage matrix elements from the homogeneous and non-homogeneous conductivity distributions. See (5.21) for the formal definition

j	depth	E_j^∞	$\mathcal{N}_j^\varepsilon$
1	22%	6.5%	120
2	44%	0.8%	116
3	67%	0.2%	20
4	89%	0.1%	2

Table 5.1: Quantitative results of the EIT ill-posedness demonstration. See Figure 5.16 for the four examples. Explanation for column "depth": since our grid is 9×9 pixels wide, the deepest point (center) is 4.5 pixel widths from the boundary. Our examples have inclusions at depths 1,2,3,4 pixel widths, which we express as percentage of the maximum depth in the table. The relative error E_j^∞ is defined in (5.21). For the $\mathcal{N}_j^\varepsilon$ column, we choose $\varepsilon = 0.002$ in (5.22). The table lists the number of data points that are above the noise level; remember that the total number of elements in these voltage matrices is 992.

5.3 EIT reconstruction by linearization

Sections 5.1 and 5.2 above introduced the context of probing nonhomogeneous conductivity distributions with electrical currents. Now it is time to turn our attention to the relevant inverse problem: given the voltage matrix $\mathbf{U}_\gamma$ of a conductivity γ, recover γ.

We know from Section 5.2.2 that $\mathbf{U}_\gamma$ depends on γ in a nonlinear way, and from Section 5.2.3 that some information about γ is encoded into $\mathbf{U}_\gamma$ in a delicate manner.

In this section we build a simple EIT reconstruction algorithm based on linearization. We assume that the conductivity distribution γ is a small perturbation of the homogeneous unit conductivity:

$$\gamma = 1 + \Delta\gamma. \tag{5.23}$$

We write a nonlinear forward map taking γ to the EIT voltage matrix

$$\Phi(\gamma) = \mathbf{U}_\gamma. \tag{5.24}$$

Substituting (5.23) into (5.24) leads to the linear approximation

$$\mathbf{U}_\gamma = \Phi(\gamma) = \Phi(1 + \Delta\gamma) \approx \mathbf{U}_1 + J\Phi(1)\Delta\gamma, \tag{5.25}$$

where $J\Phi$ is the Jacobian matrix of Φ. So we arrive at the approximate equation

$$J\Phi(1)\Delta\gamma \approx (\mathbf{U}_\gamma - \mathbf{U}_1), \tag{5.26}$$

which we can solve in the least squares sense. Note that we need the measurement $\mathbf{U}_1$ of the homogeneous target.

The above derivation is quite abstract, and we need to introduce some precise definitions to implement it in practice.

5.3.1 Parametrization of the conductivity

First we need to number the conductances between pixels in a coherent way as elements in one long vector $\vec{g}$. Let's take first the horizontal neighbors. They form a $n \times (n-1)$ matrix G_γ^H, whose elements we number using one index running column-wise as shown in Figure 5.17(a). These are the first half of elements of $\vec{g}$.

The second half of $\vec{g}$ comes from conductances between vertically neighboring pixels. They form a $(n-1) \times n$ matrix G_γ^V, whose elements are numbered as in Figure 5.17(b).

(a) (b)

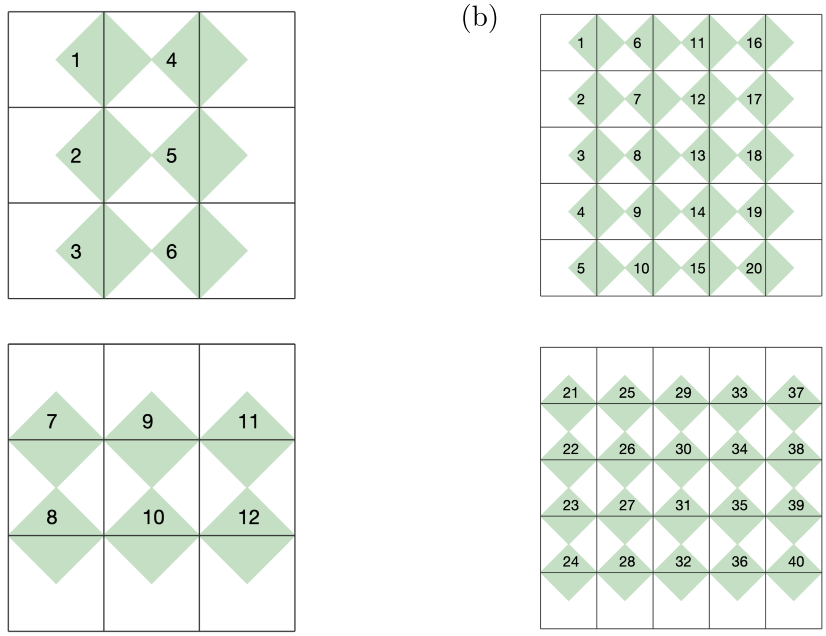

Figure 5.17: Examples of reshaping two conductance matrices into one vector. The idea is to first number the entries in the horizontal neighbors matrix column-wise with one index, and then continue the numbering in the same manner for the vertical neighbors matrix. (a) The case of 3×3 pixel grid. (b) The case of 5×5 pixel grid.

Now we have a representation of all conductances appearing in our model. The vector $\vec{g}$ has $2n^2 - 2n$ elements. Now the conceptual formula (5.23) takes the more concrete form

$$\vec{g} = \vec{1} + \Delta\vec{g} \tag{5.27}$$

with $\vec{1} = [1\ 1\ 1 \ldots 1]^T \in \mathbb{R}^M$ and the perturbation vector $\Delta\vec{g} \in \mathbb{R}^M$ assumed to be small in norm.

Note that we are still assuming that all conductances at boundary edges are equal to 1 Siemens. Modelling a more general situation would involve larger matrices and a longer vector. But we do not discuss such extensions here.

5.3.2 Forward map from adjacent current patterns

The forward map Φ for the $n \times n$ grid takes as input the conductivity vector $\vec{g}$, defined in Section 5.3.1. The output is the voltage matrix $\mathbf{U}_\gamma^{\mathrm{adj}}$ that has

n	M	N	L
3	12	56	8
5	40	240	16
7	84	552	24
9	144	992	32

Table 5.2: EIT forward map dimensions $\Phi : \mathbb{R}^M \to \mathbb{R}^N$ for a few grid sizes of $n \times n$ pixels. Note that the origin of a couple of M values is illustrated in Figure 5.17. We also include the number L of electrodes in its own column.

$L = 4(n-1)$ rows and $L-1$ columns, the latter because there are $L-1$ linearly independent current patterns. We number the elements of U again column-wise with one index, describing a vector $\vec{u}$ with length $4(n-1)(4(n-1)-1) = 16n^2 - 36n + 20$.

The domain and target spaces for the nonlinear mapping Φ thus are

$$\Phi : \mathbb{R}^{n(n-1)} \times \mathbb{R}^{n(n-1)} \to \mathbb{R}^{4(n-1)(4(n-1)-1)}.$$

Write it in a more compact way:

$$\begin{aligned}
&\Phi : \mathbb{R}^M \to \mathbb{R}^N, \\
&M = 2n^2 - 2n, \\
&N = 16n^2 - 36n + 20.
\end{aligned}$$

5.3.3 Jacobian matrix of the forward map

Denote $\vec{g} = [g_1, g_2, g_3, \ldots, g_M]^T$ and

$$\Phi(\vec{g}) = \begin{bmatrix} \Phi_1(g_1, \ldots, g_M) \\ \Phi_2(g_1, \ldots, g_M) \\ \vdots \\ \Phi_N(g_1, \ldots, g_M) \end{bmatrix}.$$

The Jacobian matrix of Φ is given by

$$J\Phi = \begin{bmatrix} \frac{\partial \Phi_1}{\partial g_1} & \cdots & \frac{\partial \Phi_1}{\partial g_M} \\ \vdots & \ddots & \vdots \\ \frac{\partial \Phi_N}{\partial g_1} & \cdots & \frac{\partial \Phi_N}{\partial g_M} \end{bmatrix}. \tag{5.28}$$

In our numerical tests we evaluate the Jacobian using a simple finite difference approach. Take $h > 0$ and denote

$$\Delta_1 = [1 + h\ 1\ 1 \dots 1]^T \in \mathbb{R}^M.$$

We calculate the first column in (5.28) as the finite difference quotient

$$\frac{\Phi(\Delta_1) - \Phi(\vec{1})}{h}.$$

The rest of the columns are computed similarly.

5.3.4 Reconstruction

From (5.27) we have $\vec{g} = \vec{1} + \Delta\vec{g}$. Then the conceptual formula (5.26) takes the concrete form

$$\Delta\vec{g} \approx (J\Phi(1))^{\dagger}(\mathbf{U}_g^{\text{adj}} - \mathbf{U}_1^{\text{adj}}) \tag{5.29}$$

with $(J\Phi(1))^{\dagger}$ the Moore-Penrose pseudoinverse of the Jacobian evaluated at conductivity vector $\vec{1}$.

We expect (5.29) to yield reasonable reconstructions when the perturbation $\Delta\vec{g}$ of the conductivity is not too large. Let's see with numerical examples how that assumption fares in a simulated test environment.

Numerical tests in the 3×3 grid

Our first test conductivity has the same overall form than the left one in Figure 5.12 related to our nonlinearity study in Section 5.2.2. However, here we take the deviation from background unity conductance to be smaller. So the resistive inclusion in the top now has conductivity 0.9 SIemens, and the bottom inclusion has conductance 1.2 Siemens, slightly higher than background. See Figure 5.18(a) for the exact conductances between the pixels.

We simulate the voltage matrices $\mathbf{U}_1^{\text{adj}}$ for the background and $\mathbf{U}_g^{\text{adj}}$ for the perturbed conductivity. Then we use formula (5.29) to reconstruct the conductivity. The result is pretty good, as you can see in Figure 5.18(b).

We derived formula (5.29) under the assumption that the conductivity is close to the background of one. What happens if this assumption is violated? To study this we repeat the above test with a higher-contrast conductivity shown in FIgure 5.19(a). Now the linearized reconstruction fails badly, even in this low-resolution model of just 3×3 pixels. We conclude that linearization is not the way to go in general for nonlinear inverse problems.

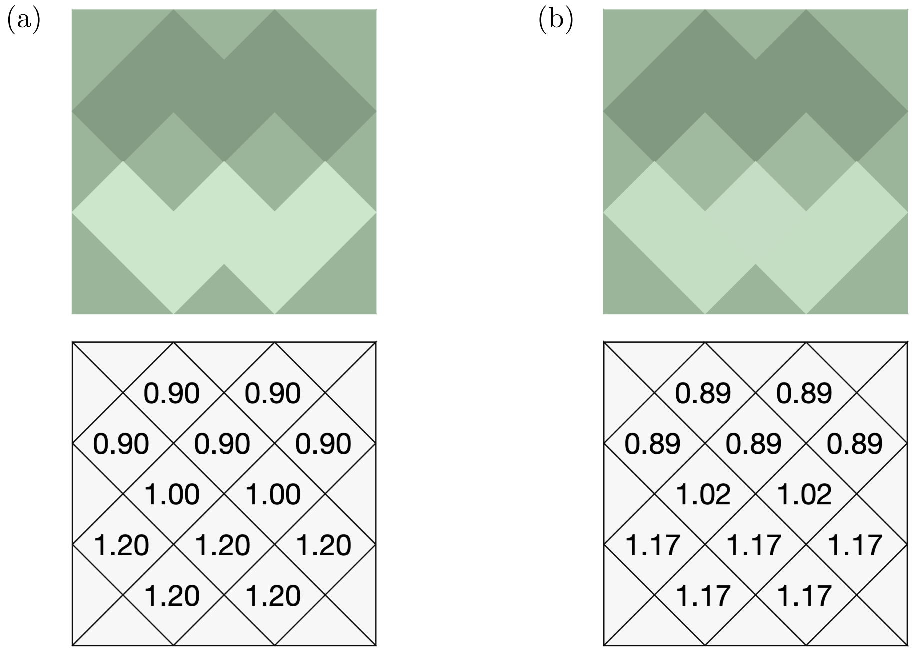

Figure 5.18: (a) Original conductivity shown in color (top) and by numbers (bottom). (b) Linearized reconstruction using (5.29), with colorscale of the top image identical to that of (a). The numbers show that we get a reasonable reconstruction accuracy.

(a) (b)

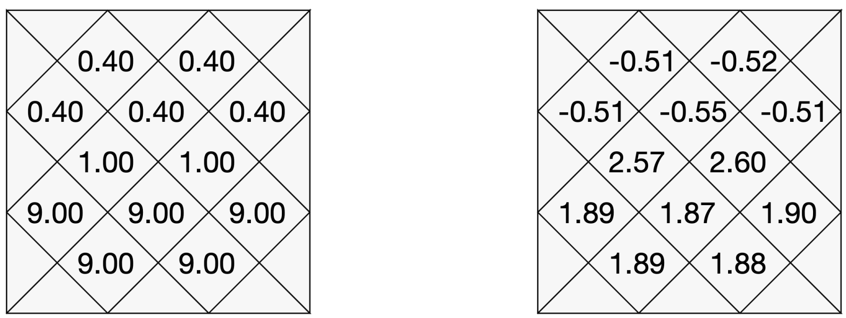

Figure 5.19: (a) Original conductivity in the 3×3 pixel grid with a large perturbation from the background conducivity of one. (b) Linearized reconstruction by (5.29) fails badly, even producing non-physical negative conductance values. Compare to the small perturbation case shown in Figure 5.18.

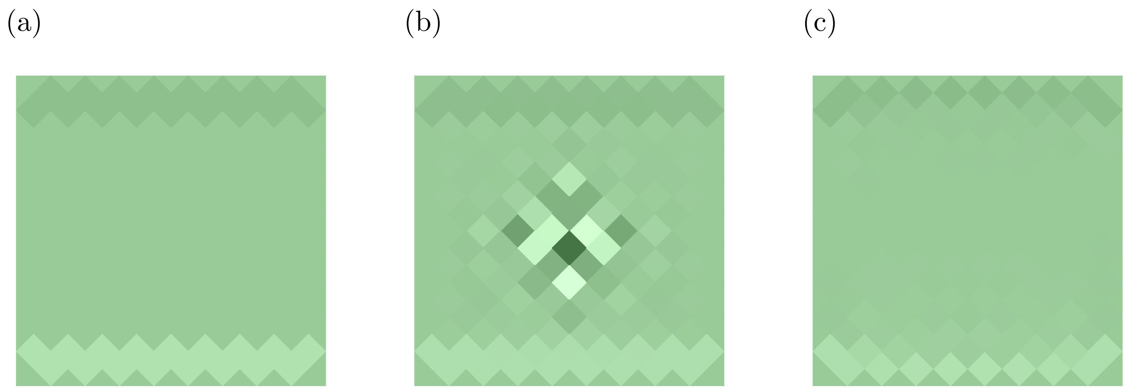

Figure 5.20: (a) Original conductivity in the 9×9 pixel grid. This is a small contrast case, with minimum conductance 0.9 Siemens and maximum 1.2 Siemens. (b) Linearized reconstruction. (c) Linearized reconstruction using a tolerance setting for the singular values in the pseudoinverse of the Jacobian.

Numerical tests in the 9×9 grid

How does the linearized EIT reconstruction formula (5.29) perform at higher-dimensional models when the conductivity contrast is small? Let's test that with a 9×9 pixel grid. We again take inclusions with conductivity 0.9 SIemens and 1.2 Siemens; see Figure 5.20(b).

We observe from Figure 5.20(b) that higher resolution presents difficulties for formula (5.29) even in the case of small perturbations. We found in Section 5.2.3 that EIT has a harder time seeing deeper into the domain, and the artefacts in the middle of the reconstruction shown in 5.20(b) are compatible with that finding.

One trick around that problem is to use a tolerance for singular values in the use of pseudoinverse in (5.29). See Figure 5.20(c).

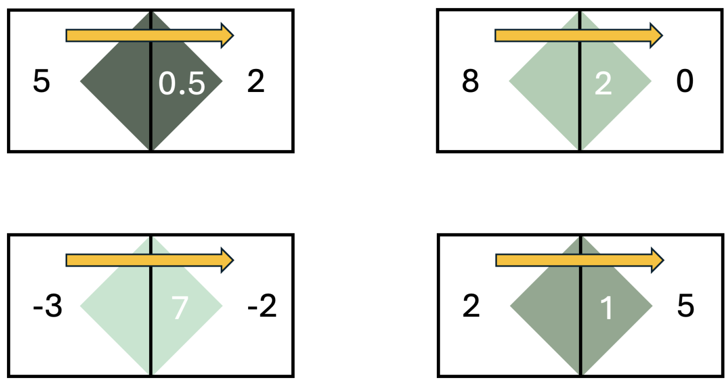

Figure 5.21: Current flow problems.

5.4 Exercises

5.4.1 Currents between pixels

calculate the current flowing from the left pixel to the right pixel in the examples shown in Figure 5.21. Note that the result can be a negative number. In that case the direction of current flow is against the arrow direction.

5.4.2 Longer 1D diffusion models

(a) Write a program solving the general n-pixel one-dimensional diffusion model when conductances are given for each edge between pixels.

(b) Can you prove that the matrix has a one-dimensional kernel?

5.4.3 General equation for the three-pixel case

Write the matrix system (5.7) for the case of general conductances $G_\ell > 0$ with $\ell = 0, 1, 2, 3$.

5.4.4 Further evidence for non-uniqueness

Form another inhomogeneous conductive rod (in addition to those in Figure 5.6) that produces the same 3.2 mV measurement than reported in Figures 5.7 and 5.8. By “form,ing a rod” we mean choosing suitable values for G_1 and G_2. Check the result computationally by either modifying the routine `FD_EIT_1D_demo_case3.m` or by writing your own solution code.

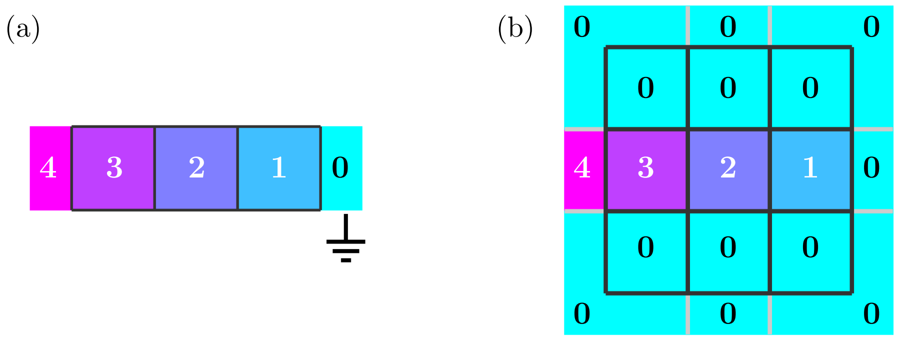

Figure 5.22: (a) Voltages and currents in the homogeneous one-dimensional diffusion model discussed in Section 5.1.2. The voltages are indicated in the pixelized rod. (b) Artificial values for the voltage variables to be analyzed in the exercise.

5.4.5 Voltage-to-current measurement

TO DO

5.4.6 The difference between 1D and 2D

Recall the one-dimensional homogeneous diffusion model of Section 5.1.2. The solution is shown in Figure 5.22(a). Inspired by the straight-shooting X-rays, one could imagine the two-dimensional homogeneous diffusion model to have the solution shown in Figure 5.22(b), where the electric current is simply traveling through the square in the middle. Here the idea is to feed 1mA of surrent into the square through the "nine o'clock pixel" and take the current out through the "three o'clock pixel". In this case the one-dimensional solution would just be embedded into the two-dimensional model, with all the rest of the voltages being zero.

Your task is to find out why the numbers in Figure 5.22(b) are non-physical. More precisely, find one or more pixels where the balance equation (5.11) fails.

5.4.7 Skip patterns

TO DO

5.4.8 Nonlinearity study

Let one internal conductance G range from 0.1 to 10. Fix a current pattern. Plot some of the measured voltages as function of G. What do you observe?

5.4.9 Reconstruction exercise

TO DO

5.4.10 Two-dimensional voltage-to-current measurement

TO DO

Part II

Inverse problems in medical imaging

Part III

Spotlight on electrical impedance tomography

Part IV

Application-driven inversion methods